



저작자표시-비영리-변경금지 2.0 대한민국

이용자는 아래의 조건을 따르는 경우에 한하여 자유롭게

- 이 저작물을 복제, 배포, 전송, 전시, 공연 및 방송할 수 있습니다.

다음과 같은 조건을 따라야 합니다:



저작자표시. 귀하는 원저작자를 표시하여야 합니다.



비영리. 귀하는 이 저작물을 영리 목적으로 이용할 수 없습니다.



변경금지. 귀하는 이 저작물을 개작, 변형 또는 가공할 수 없습니다.

- 귀하는, 이 저작물의 재이용이나 배포의 경우, 이 저작물에 적용된 이용허락조건을 명확하게 나타내어야 합니다.
- 저작권자로부터 별도의 허가를 받으면 이러한 조건들은 적용되지 않습니다.

저작권법에 따른 이용자의 권리는 위의 내용에 의하여 영향을 받지 않습니다.

이것은 [이용허락규약\(Legal Code\)](#)을 이해하기 쉽게 요약한 것입니다.

[Disclaimer](#)

의학석사 학위논문

Anterior Tenting vs. Wrapping  
Technique for Acellular Dermal  
Matrix in Breast Reconstruction  
Under Post-mastectomy  
Radiotherapy in Rats

방사선 조사 유방재건 랫드 모델에서 무세포성  
진피 기질 피복 방법에 따른 비교

2023 년 8 월

서울대학교 대학원

의학과 성형외과학 전공

김 지 영

Anterior Tenting vs. Wrapping Technique  
for Acellular Dermal Matrix in Breast  
Reconstruction Under Post-mastectomy  
Radiotherapy in Rats

지도 교수 진 응 식

이 논문을 의학석사 학위논문으로 제출함

2023 년 4 월

서울대학교 대학원

의학과 성형외과학 전공

김 지 영

김지영의 의학석사 학위논문을 인준함

2023 년 7 월

위 원 장 장 학 (인)

부위원장 진 응 식 (인)

위 원 이 한 별 (인)

Abstract

Anterior Tenting vs. Wrapping  
Technique for Acellular Dermal  
Matrix in Breast Reconstruction  
Under Post–mastectomy  
Radiotherapy in Rats

Ji–Young Kim

School of Medicine

Major in Plastic and Reconstructive Surgery

The Graduate School

Seoul National University

Background: Implant–based reconstruction with acellular dermal matrix (ADM) is an increasingly popular breast reconstruction method. Anterior tenting and wrapping are typical ADM placement techniques in prepectoral breast reconstruction. This study aimed to compare the outcomes of these two surgical techniques.

Methods: Fifteen rats were divided into three groups: control (n=5), anterior tenting (n=5), and whole wrapping (n=5). Two 1.5 cm–diameter silicone implants were inserted in each rat. Only silicone implants were placed in the control group. The anterior surface of the implants was

covered with ADM in the anterior tenting group, whereas the implants were fully wrapped with ADM in the whole wrapping group. Animals were irradiated on one side of the back three weeks postoperatively and sacrificed three months postoperatively. Tonometry was performed to measure the tension of the implant pocket. Histopathological analysis was conducted on the capsule surrounding the implant and the ADM.

Results: During the experiment, one rat from the control group died, and analysis was conducted on a total of 14 animals. The range of change in tonometry values with or without irradiation in whole wrapping tended to be larger than that of anterior tenting ( $p=0.008$ ). The cellular capsule was significantly thinner on the side covered by ADM (anterior side,  $p=0.029$ ; posterior side,  $p=0.037$ ). There were no significant differences observed in the other microscopic features of the cellular capsule. The microscopic analysis of ADM revealed significant increases in total capsule thickness ( $p=0.024$ ) and collagen density ( $p=0.015$ ) with radiation exposure, while a significant decrease was observed in  $\alpha$ -SMA positive area ( $p=0.009$ ) and CD3 positive cells ( $p=0.025$ ).

Conclusion: The whole wrapping technique exhibited a greater increase in intraprosthetic pressure due to structural changes in ADM caused by radiation, compared to the anterior tenting technique. Therefore, in patients with the possibility of adjuvant radiation therapy, the anterior tenting technique is recommended over whole wrapping.

**Keywords : breast reconstruction, acellular dermal matrix, radiation, capsular contracture**

**Student Number : 2021–29067**

# Contents

Abstract .....	i
Contents .....	iii
Introduction .....	1
Methods.....	4
Results .....	10
Discussion.....	15
Conclusions .....	19
Figure and table.....	20
References .....	33
Abstract in Korean .....	38

# Introduction

Breast cancer is the most prevalent cancer among women, accounting for 30% of all cancers in women in 2021.<sup>1</sup> Breast reconstruction is a procedure performed to restore the breast after mastectomy. Reconstructive surgeons have been seeking reconstruction methods that can achieve natural-looking results with fewer surgeries and less invasiveness. Prepectoral implant-based breast reconstruction has emerged as a promising approach<sup>2</sup> as it involves advanced techniques such as nipple-sparing mastectomy<sup>3</sup> and the use of acellular dermal matrix (ADM) along with high-quality implants.

ADM, which is derived from various sources including humans, pigs, and cows, is primarily composed of collagen and elastin fibers.<sup>4</sup> The production of ADM involves a process called decellularization, which is designed to remove cellular components. Over time, ADM can integrate into the surrounding tissue and become a permanent part of the body.<sup>5</sup> In addition to its biocompatibility, it can be easily molded according to the shape of the reconstruction site. When ADM is used in breast reconstruction, it has a lower pole stretching effect and serves to support the structure. It is also known to reduce capsular contractures.<sup>6</sup>

Capsular contracture, the excessive growth of fibrous tissue around breast implants, is a common complication that can cause discomfort, deformity, and implant displacement. Capsular contracture remains a

significant challenge in breast reconstruction, affecting a considerable percentage of individuals, with reported prevalence rates ranging from 13.7% to 45%.<sup>7</sup> The occurrence of capsular contracture is influenced by various factors, including radiation therapy, implant texture, bacterial contamination, surgical site infections, and hematoma.<sup>8-10</sup> Notably, adjuvant radiation therapy is a significant risk factor, with reported rates of capsular contracture reaching up to 40% in patients receiving post-mastectomy radiotherapy.<sup>11</sup>

Radiation also affects ADM as it can alter collagen structure and inhibit the integration of ADM in the periprosthetic area. While ADM serves as a barrier against contracture, unsuccessful integration may lead to ADM-associated contracture.<sup>12</sup> In this regard, there is no consensus on the optimal use of ADM in implant-based breast reconstruction.

Various methods have been used to cover implants with ADM. In addition to the wrapping technique that covers the entire surface of the implant, the anterior tenting technique that covers the front surface of the implant in contact with the mastectomy skin flap is widely used. In clinical practice, a study has reported no significant difference in complications between the anterior-tenting and whole-wrapping techniques.<sup>13</sup> However, another study has suggested that using a larger ADM, rather than a thicker one, may increase the drainage volume and duration, which could potentially increase the risk of seroma or infection.<sup>14</sup> However, the specific differences between these techniques

remain unclear, and the selection of the coverage method often relies on surgeons' preferences.

Our study aimed to examine the impact of radiation on ADM and compare the outcomes between the anterior tenting and whole wrapping technique in terms of their potential impact on intraprosthetic pressure, which serves as an indicator for capsular contracture. Through this investigation, we hope to gain a better understanding of the risks and benefits associated with ADM use in breast reconstruction and to inform clinical decision-making to optimize patient outcomes.

# Method

The experiments were carried out at the Biomedical Research Institution of Seoul National University Hospital (IACUC approval number 22-00770-S1A1). Fifteen 8-week-old male Sprague-Dawley rats were randomly divided into three groups according to the implant coverage technique: control (n=5), whole wrapping (n=5), and anterior tenting (n=5) (Fig 1).

## **Surgical procedure**

Smooth-type hemispherical implants with a diameter of 1.5 cm were prepared. Non-meshed ADM (BellaCell HD, Hans Biomed Corp., Seongnam, Korea) with thickness of 1.8-2.99 mm was used. The animals were subjected to general anesthesia with 3% isoflurane. Xylazine (5 mg/kg) was intramuscularly administered. They were maintained under controlled ventilation with 1-1.5% isoflurane. A prophylactic dose of cefazolin (120 mg/kg/dose) was also administered intraperitoneally after adequate anesthesia was achieved. After shaving the dorsum of each animal, skin preparation was performed with betadine in a sterile fashion. We dissected two pockets at the back of each rat: one left and one right of the midline. Each animal received two implants below the panniculus carnosus. In the whole wrapping group, the implant was covered by the ADM *ex vivo* secured with absorbable sutures (4-0

Monosyn), and the unit was secured using a 3–0 Vicryl suture at the 6 o’ clock position. In the anterior tenting group, the ADM was placed over the skeletal muscle of the back and secured using three cardinal sutures at 12, 3, and 9 o’ clock positions with a 3–0 Vicryl suture to form a pre–muscle pocket. After implant insertion, the pocket was closed with a 3–0 Vicryl suture at the 6 o’ clock position.

### **Radiation protocol**

The aim of our radiation protocol was to simulate the effects of adjuvant irradiation following mastectomy. For experimental purposes, the recommended radiation dose typically ranges between 14 and 25 Gy.<sup>15</sup> In clinical practice, the conventional radiotherapy protocol delivers a total dose of 50 Gy in 25 fractions of 2 Gy to the chest wall. By using the linear–quadratic concept, we can compare the tissue effects of different fractionation regimes. This allows us to calculate the biological effective dose (BED) and determine that our radiation protocol yields a similar BED to conventional radiation therapy.<sup>16</sup> In our study, the total dose of 23.25 Gy was divided into three fractions of 7.75 Gy each, administered over a period of 5 days. One of the two implantation sites for each animal was randomly selected and irradiated externally using a 6–MeV electron beam collimated by a 6×6 cm cone at a source–to–surface distance of 100 cm (VitalBeam, Varian, USA) 3 weeks after surgery.

### **Applanation Tonometry**

At the three-month follow-up after surgery, the animals underwent intraprosthetic pressure evaluation using applanation tonometry. Tonometry has been effectively utilized to measure the pressure within the mammary glands.<sup>17</sup> Tonometry was performed as described by Moore in 1979.<sup>18</sup> A glass disc with a diameter of 5 cm and thickness of 2.5 mm was placed on the skin at the location of the implant. The skin was marked with gouache paint and a sheet of paper was placed between the glass disc and the painted skin surface. The flattened area was calculated using ImageJ software. It is expected that a larger flattened area would indicate lower tension within the implant pocket.

### **Histopathologic analysis**

The animals were then euthanized through exposure to high concentrations of carbon dioxide 3 months postoperatively. The tissues were removed by cutting the skin along the curved surface of the implant. In the control group, specimens were collected, including the panniculus carnosus. In the group where the implant was covered with ADM, specimens were obtained as a whole, including the ADM. The collected tissues were then fixed for histological examination. Histopathological analysis was performed on the capsules to assess capsule thickness, collagen density, myofibroblast, and inflammation. Each sample with the

implant in place was fixed in 10% buffered formalin. After fixation, the capsules were separated from the implants and carefully embedded in paraffin blocks. All specimens were taken, including the whole aspect (anterior and posterior surfaces) of the capsule and ADM at the midline (Fig 2). The properties of the capsule and ADM were examined by categorizing them based on their respective orientations. This involved examining the anterior surface, where the ADM was in contact with the skin flap, and the posterior surface, where the ADM interacted with the underlying skeletal muscle. The specimens were examined histologically for thickness and collagen density, and immunohistochemical staining was used to examine the  $\alpha$ -smooth muscle actin ( $\alpha$ -SMA) positive area and the CD3-positive cell count. Three areas were analyzed for each anterior and posterior surface. To quantify the area of the region of interest, which was stained, ImageJ software was used for quantitative analysis. For the evaluation of the cellular capsule, a region of 0.01 mm<sup>2</sup> was analyzed. Similarly, for the assessment of ADM, a region of 0.102 mm<sup>2</sup> was analyzed.

*(1) Hematoxylin and eosin staining*

Sections (5-  $\mu$ m thick) were cut and stained with hematoxylin and eosin to examine their histopathological characteristics. Using the NIKON ECLPSE Ci-L microscope, the thickness of the total capsule and the cellular capsule were evaluated. The cellular capsule refers to the

parallel layers of collagen fibers that forms at the interface between the ADM and the implant. In contrast, the total capsule refers to the complete implant pocket, including the ADM, which is excised as a whole during the surgical procedure (Fig 3).

### *(2) Masson' s trichrome staining of collagen fibers*

Another set of capsule samples was stained with Masson' s trichrome after fixation in 10% formalin solution for 24 h. Samples were sectioned into 5-  $\mu$ m sections. The collagen fibers were stained blue, the nuclei were stained black, and the background was stained red. The stained collagen fiber area was quantified per respective region as collagen density using ImageJ software.

### *(3) Immunohistochemistry for $\alpha$ -SMA and CD3*

The level of myofibroblast involvement in the capsule and ADM was examined using the anti-SMA antibody as the primary antibody. Meanwhile, the CD3 antibody was used as the primary antibody to determine the degree of inflammation by examining T cell count. Tissue sections were cut and mounted on slides and then stained using the Discovery XT automated immunohistochemistry stainer (Ventana Medical Systems, Inc., Tucson, AZ, USA).  $\alpha$ -SMA positive myofibroblasts were calculated as the  $\alpha$ -SMA positive area per

respective region. The number of CD3 positive cells per respective region was counted using the NIKON ECLPSE Ci-L microscope.

### **Statistical Analysis**

Data are expressed as mean  $\pm$  SD for continuous variables. Generalized estimating equations (GEE) were used to verify the interaction between the therapy factor (coverage technique and radiation) and result variables (tonometry, capsule thickness, collagen density, level of  $\alpha$ -SMA, and CD3 positive cell count). The interaction effect (Group \* radiation status) was assessed, and if no significant interaction was found, the significance of each factor (Group and radiation status) was evaluated after removing the interaction effect. Statistical significance was considered at  $p < 0.05$ . In cases where the GEE analysis revealed statistical differences among the groups, post-hoc analysis was performed using Bonferroni correction (adjusted for  $p < 0.05$ ). All analyses were performed using SAS statistical software (SAS system for Windows, version 9.4; SAS Institute, Cary, NC).

# Result

Samples were obtained three months after the surgical procedure; however, one rat from the control group expired prematurely during anesthesia for irradiation. Therefore, the analysis was conducted on a total of 14 animals, with four in the control group, five in the whole wrapping group, and five in the anterior tenting group.

## **Intraoperative Pressure**

The tonometry results exhibited different patterns among groups depending on whether irradiation was performed ( $p = 0.008$ ) (Fig 4). A post hoc analysis was conducted to determine which group showed a significant difference. In the absence of radiation, a significant difference in tonometry results was observed only between the control and anterior tenting groups ( $p=0.039$ ); however, in the presence of radiation, the tonometry results were significantly higher in the control and whole wrapping groups compared with the anterior tenting group (control vs. anterior tenting,  $p=0.023$ ; whole wrapping vs. anterior tenting,  $p<0.001$ ). The increase in tonometry results tended to be larger in the whole wrapping group than in the anterior tenting group under irradiation.

## **Histopathologic finding**

The differences in cellular capsules and ADM for each coverage method were evaluated (Fig 5–8.)

*Characteristics of the cellular capsule (Table 1, 2)*

*(1) Cellular capsule thickness*

When analyzing the anterior and posterior capsule thickness separately, no statistically significant interaction was observed between the groups and irradiation (anterior side,  $p=0.472$ ; posterior side,  $p=0.331$ ). However, there was a significant difference between the groups in terms of capsule thickness (anterior side,  $p=0.029$ ; posterior side,  $p=0.037$ ) (Fig 9A, 9B), and irradiation did not cause a significant difference in capsule thickness (anterior side,  $p=0.107$ ; posterior side,  $p=0.067$ ). Post-hoc analysis showed that anterior capsule thickness was significantly different between the control group and both the whole wrapping group ( $p<0.0001$ ) and the anterior tenting group ( $p<0.0001$ ), but there was no significant difference between the anterior tenting and whole wrapping groups. In terms of posterior capsule thickness, there was a significant difference among all the groups (control vs. whole wrapping,  $p<0.0001$ ; control vs. anterior tenting  $p=0.021$ ; whole wrapping vs. anterior tenting,  $p<0.0001$ ).

*(2) Collagen density*

Upon examining whether the results of capsule collagen density exhibited different patterns between groups depending on whether irradiation was conducted, no statistically significant difference was found (anterior side,  $p=0.241$ ; posterior side,  $p=0.702$ ). There was no significant difference between the groups in terms of collagen density (anterior side,  $p=0.112$ ; posterior side,  $p=0.081$ ) and according to irradiation status (anterior side,  $p=0.289$ ; posterior side,  $p=0.112$ ) (Fig 9C, 9D).

### (3) Immunohistochemistry result

Regarding the  $\alpha$ -SMA positive area, interaction between coverage method and irradiation did not exist (anterior side,  $p=0.611$ ; posterior side,  $p=0.603$ ). Additionally, there were no significant differences between the groups in the  $\alpha$ -SMA positive area for both the anterior surface ( $p = 0.164$ ) and the posterior surface ( $p = 0.077$ ). Likewise, there were no significant differences in the  $\alpha$ -SMA positive area based on irradiation for both the anterior surface ( $p = 0.246$ ) and the posterior surface ( $p = 0.054$ ) (Fig 9E, 9F).

Regarding the CD3-positive cell count, no significant interaction was observed between radiation and the coverage method (anterior side,  $p=0.097$ ; posterior side,  $p=0.104$ ). Similarly, there were no significant differences between the groups in terms of the CD3-positive cell count for both the anterior surface ( $p = 0.371$ ) and the posterior surface ( $p =$

0.646). Furthermore, no significant differences in the CD3-positive cell count were observed based on irradiation for both the anterior surface ( $p = 0.581$ ) and the posterior surface ( $p = 0.491$ ) (Fig 9G, 9H).

### *Characteristics of ADM*

The analysis of ADM was divided into three groups based on the location of the obtained capsule samples, considering the coverage method and the orientation of the capsule. These groups consisted of the anterior and posterior sides of the capsule in the whole wrapping group, and the anterior side of the capsule in the anterior tenting group (Table 3). There was no significant interaction between the sampling side and radiation in the analysis of each result. Additionally, no significant differences were observed among the groups for any of the analyzed variables. However, radiation had a significant impact on all variables (Table 4).

#### (1) Total capsule thickness

The result of total capsule thickness (Mean $\pm$ SD) across all samples was  $1504.36\pm 704.94$   $\mu\text{m}$ . In the non-radiated group, the thickness was  $1239.85\pm 581.53$   $\mu\text{m}$ , while in the radiated group, it was  $1768.86\pm 735.72$   $\mu\text{m}$ . A significant increase in total capsule thickness was observed after radiation ( $p=0.024$ ) (Fig 10A).

## (2) Collagen density

The result of collagen density of ADM (Mean±SD) was  $53.59 \pm 6.81\%$  across all samples. In the non-radiated group, the mean density was  $48.98 \pm 5.00\%$ , while in the radiated group, it was  $58.20 \pm 5.04\%$ . A significant increase in collagen density was observed after radiation ( $p=0.015$ ) (Fig 10B).

## (3) Immunohistochemistry result

The result of  $\alpha$ -SMA positive area (Mean±SD) was  $5.20 \pm 1.81\%$  across all samples. In the non-radiated group, the mean area was  $6.29 \pm 1.52\%$ , while in the radiated group, it was  $4.11 \pm 1.39\%$ . The result of CD3 positive cell count (Mean±SD) was  $30.77 \pm 12.09$  cells/ $0.102\text{mm}^2$  across all samples. In the non-radiated group, the mean count was  $35.53 \pm 10.29$  cells/ $0.102\text{mm}^2$ , while in the radiated group, it was  $26 \pm 12.17$  cells/ $0.102\text{mm}^2$ . In the radiated group, there was a lower infiltration of cells within the ADM, and both the  $\alpha$ -SMA positive area ( $p=0.009$ ) and CD3 positive cell count ( $p=0.025$ ) were significantly lower compared to the non-radiated group (Fig 10C, 10D).

## Discussion

Since ADM was first applied with split thickness skin graft to burn wounds by Wainwright in 1995,<sup>12</sup> various types of ADM, such as meshed<sup>19</sup> and diced<sup>20</sup>, have been manufactured to improve applicability. In the field of breast surgery, ADM is used for revision of capsular contracture<sup>21</sup> or plays a role in supporting the implant during implant-based breast reconstruction, and it is believed to be effective in reducing capsule formation.<sup>6,22</sup>

The occurrence of capsular contracture involves three essential components: a thick capsule characterized by collagen fibers aligned in a parallel orientation and a significant presence of contractile myofibroblasts.<sup>23</sup> Previous research has demonstrated that the cellular capsule formed at the ADM-implant interface is thinner compared to the muscle-implant interface,<sup>6, 24</sup> with lower levels of myofibroblasts, fibroblasts, vascularity, and macrophages.<sup>6</sup> The uninterrupted parallel alignment of collagen fibers creates a stronger force of contracture.<sup>25</sup> In this study, we compared two groups: one where the entire implant was wrapped and another where only the anterior surface was covered. No significant differences were found between the groups for the anterior surface, except in the control group. However, for the posterior surface, the control group had the highest thickness, followed by the anterior tenting group, and then the whole wrapping group. Consistent with

previous research, our findings demonstrate reduced capsule formation on the side covered with ADM. Additionally, our results suggest that using ADM to define the implant pocket can act as a physical barrier, preventing host cell entry and contributing to the reduction of capsule formation even without direct implant coverage in the anterior tenting technique. However, at 3 months post-surgery, the cellular capsule was very thin to cause contracture, and the overall cell presence was not significantly high. Apart from thickness, no statistically significant numerical differences were observed in the characteristics of the cellular capsule.

Radiation exposure impacts ADM by altering the structure of collagen and impeding its integration in the surrounding area of the implant. A study found that when ADM was used for whole wrapping of the implant and radiation was administered, there was a notable decrease in cellular invasion within the irradiated ADM compared to non-irradiated ADM.<sup>26,</sup>

<sup>27</sup> Previous studies have examined the structural effects of radiation on collagen materials, specifically in relation to cross-linking induction. The use of e-beam irradiation prompts cross-linking in collagen fibers, resulting in improved mechanical strength and stiffness of the collagen materials.<sup>28, 29</sup> This is attributed to the denser formation of collagen fibers, resulting in a decrease in volume. Although the specific volume change of the ADM used in our study was not measured, prior research has shown that radiation exposure at 20 Gy can lead to approximately a

70% reduction in ADM volume.<sup>29</sup> In this study, we examined the changes in ADM based on the radiation exposure status for each ADM coverage method taking into consideration the orientation of the capsules. Whether it was whole wrapping, anterior tenting, or obtained from anterior side or posterior side, radiation exposure led to a decrease in cells measured in the central region of the ADM and a denser collagen fiber network in the thicker ADM. The decrease in volume combined with an increase in thickness suggest an indirect indication of a reduction in the surface area of the implant pocket, and the surface area of the implant pocket is associated with the degree of contracture.<sup>30</sup> Under radiation, cells within the ADM were rarely observed, which correlated with lower counts of  $\alpha$ -SMA and CD3 positive cells.

When examining the pressure change of the implant pocket, as measured by tonometry, the extent of pressure changes due to radiation exposure was significantly greater in the whole-wrapping group than the anterior tenting group. When ADM was used to cover the implant, it led to a reduced formation of cellular capsule at the implant interface. However, radiation exposure led to an increase in the thickness and rigidity of ADM, accompanied by a greater decrease in the surface area of the pocket surrounding the implant. In the case of anterior tenting, the pressure resulting from these ADM changes increased in a partial area of the anterior surface of the implant. On the other hand, in the case of whole wrapping, the pressure perpendicular to the implant surface was

applied circularly throughout the entire area surrounding the implant. Therefore, tonometry values were more sensitive to radiation in the case of whole wrapping.

This study had several limitations. First, experimental comparisons in a dynamic biological environment were difficult because of the small sample size and there was only one endpoint. However, the duration of this study was considered appropriate, in comparison to previous studies that have reported neovascularization<sup>31</sup> and cellular invasion<sup>26</sup> in ADM after implantation. Another limitation of this study was that using a rat model for breast reconstruction may not fully replicate the human conditions, as placing the implant on the rat's back differs from the natural breast environment. Additionally, there may be differences in the ratio of ADM thickness to human skin thickness compared to rat skin thickness. Clinical studies are needed to validate the relevance of the research findings to human breast tension. Despite these limitations, rats are commonly used as an animal model for breast reconstruction research. Tonometry measurements of actual tension values can offer valuable insights for selecting appropriate ADM coverage methods in breast implant patients.

## Conclusions

The objective of this study was to compare the outcomes of anterior tenting and whole wrapping techniques in implant-based breast reconstruction with ADM under post-mastectomy radiation using rat model. Results from tension values showed that the range of change in the whole wrapping group tended to be larger than that of the anterior tenting group under irradiation. Histopathological examination revealed that there were no significant differences in capsule characteristics except capsule thickness. In cases where radiation exposure was administered, the recellularization of ADM was hindered, and the formation of denser collagen fibers led to a decrease in ADM volume. Moreover, the thicker ADM indicated a decrease in the implant pocket surface when considering the concomitant decrease in ADM volume. As a result, in the case of whole wrapping, where ADM fully surrounded the implant, the intraprosthetic pressure was more sensitive to radiation-induced changes in ADM compared to anterior tenting, where only a partial coverage of ADM was present. Overall, the anterior tenting technique demonstrated more resistance to radiation-induced changes in ADM compared to whole wrapping. In clinical scenarios, it is advisable to use the anterior tenting technique in implant-based breast reconstruction with ADM for breast cancer patients who may undergo postoperative radiation therapy.

# Figure and table

Figure 1. Schematic illustration of the experimental design

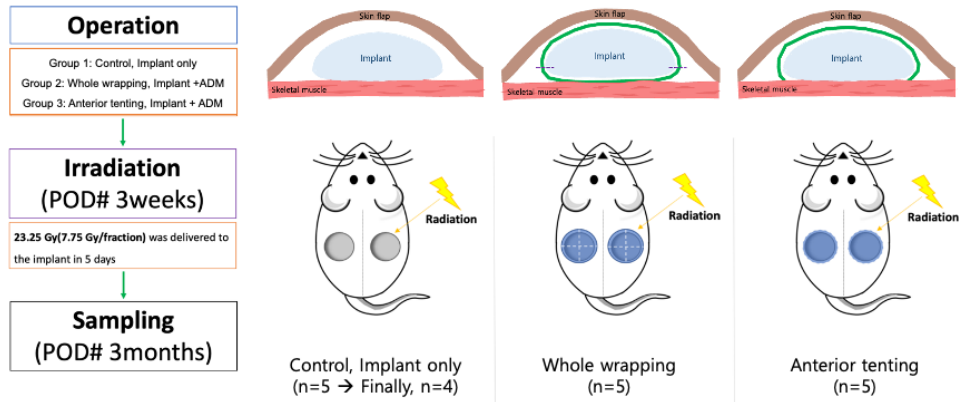
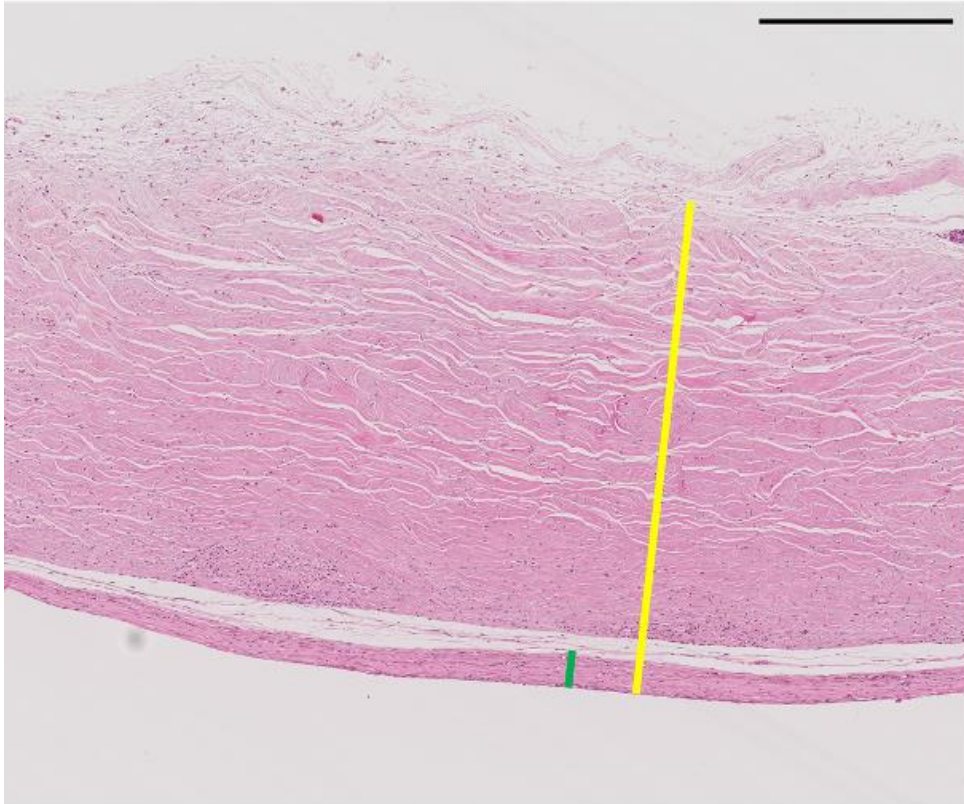


Figure 2. Gross photograph of the implant capsule in the anterior–tenting group after halving. Asterisk, anterior surface; Yellow arrow, posterior surface.

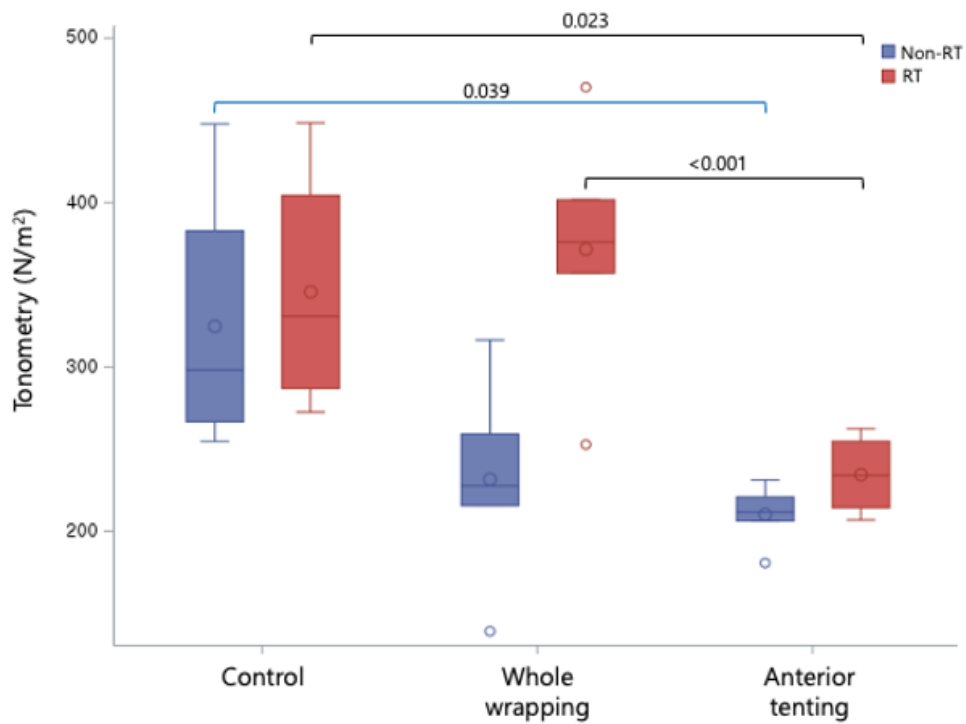


Figure 3. Measurement of capsule thickness in hematoxylin and eosin (H&E) staining. Yellow line, Total capsule thickness; Green line, cellular capsule thickness.



Scale bar: 500 $\mu$ m

Figure 4. Comparison of intraprostatic pressure (RT, Irradiation; Non-RT, Non-Irradiation).



Result	Radiation	Group			Independent of group p-value
		Control (n=4)	Whole wrapping (n=5)	Anterior tenting (n=5)	
Tonometry (N/m <sup>2</sup> , Mean±SD)	Non-RT	324.87±86.12	231.73±64.74	210.30±18.94	0.103
	RT	345.79±77.69	371.72±78.97	234.60±24.32	
Independent of radiation	p-value	0.121			0.008*

\*Interaction between the coverage method (group) and radiation

Figure 5. Hematoxylin and eosin (H&E) staining of the implant capsule of anterior side in control (*first row*), whole wrapping (*second row*), and anterior tenting (*third row*). Scale bars = 500  $\mu$  m (RT, Irradiation; Non-RT, Non-Irradiation).

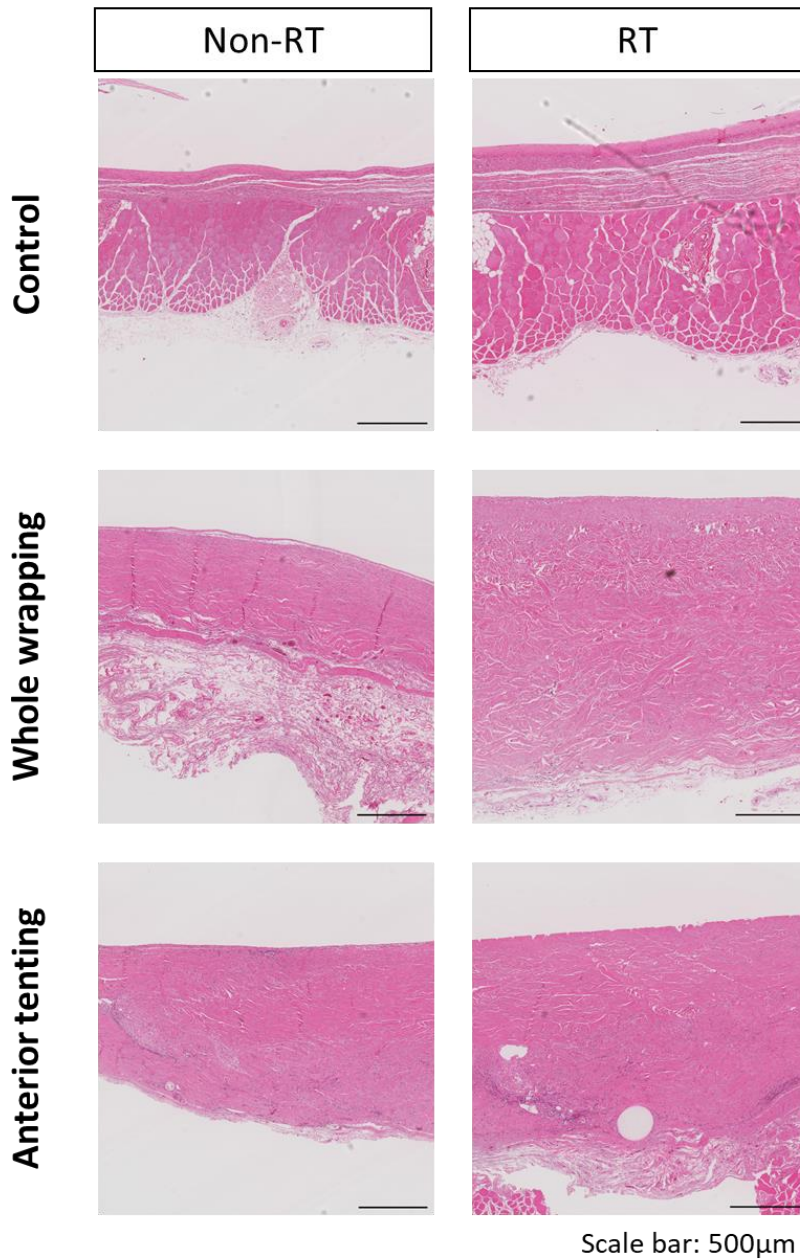


Figure 6. Hematoxylin and eosin (H&E) staining of the implant capsule of posterior side in control (*first row*), whole wrapping (*second row*), and anterior tenting (*third row*). Scale bars = 500  $\mu$ m (RT, Irradiation; Non-RT, Non-Irradiation).

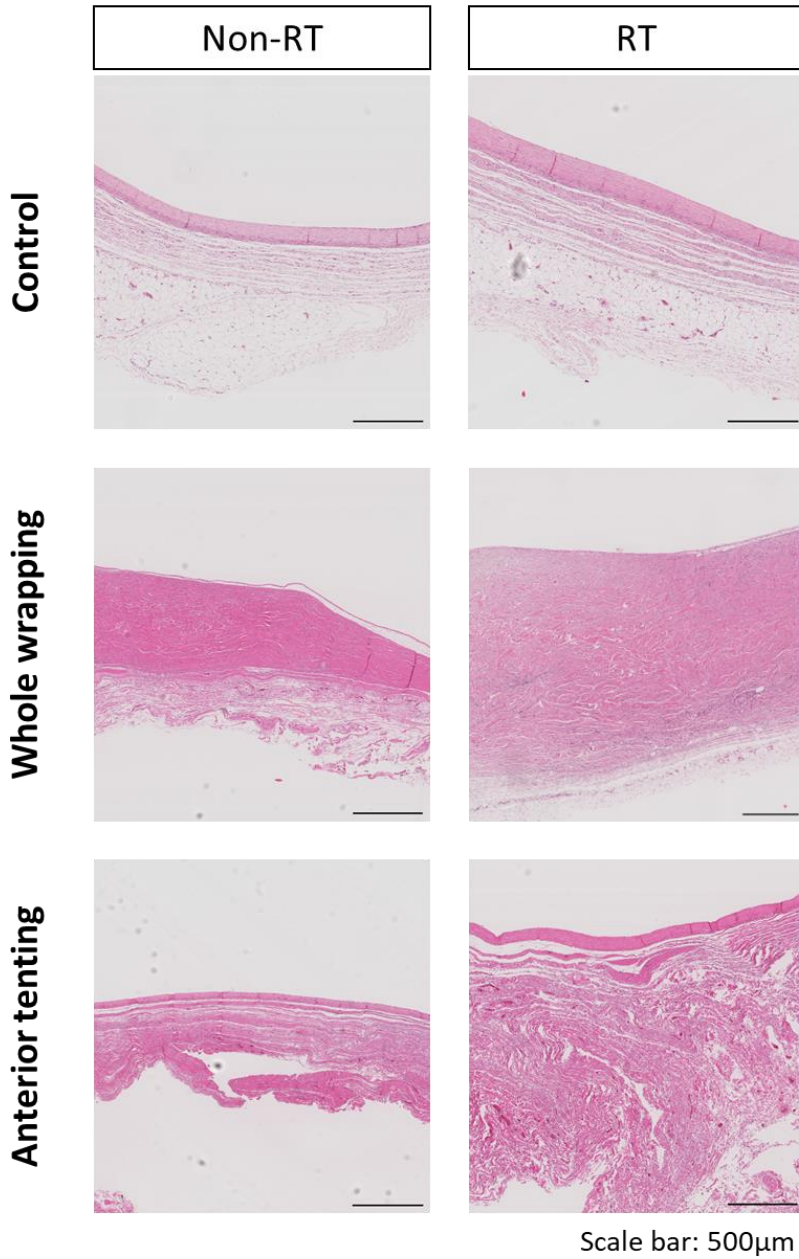


Figure 7. Masson' s trichrome staining and immunohistochemistry ( $\alpha$ -SMA and CD3) result of the implant capsule of anterior side in control (*first and second row*), whole wrapping (*third and fourth row*), and anterior tenting (*fifth and sixth row*). Scale bars = 200  $\mu$ m (RT, Irradiation; Non-RT, Non-Irradiation).

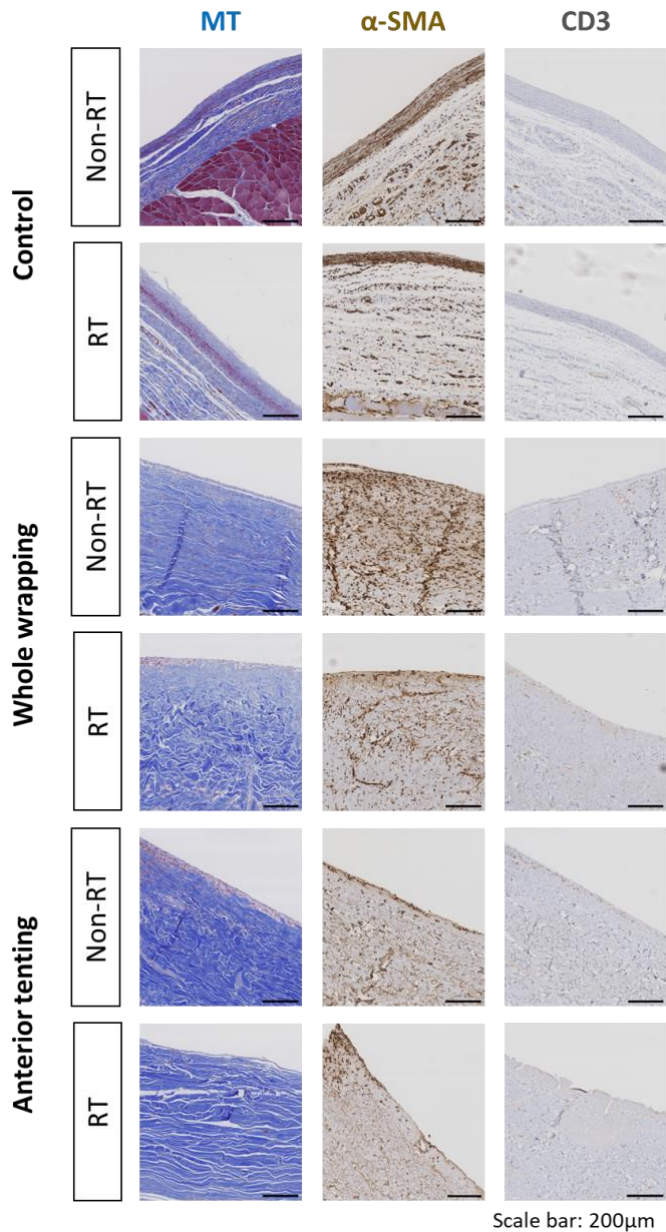
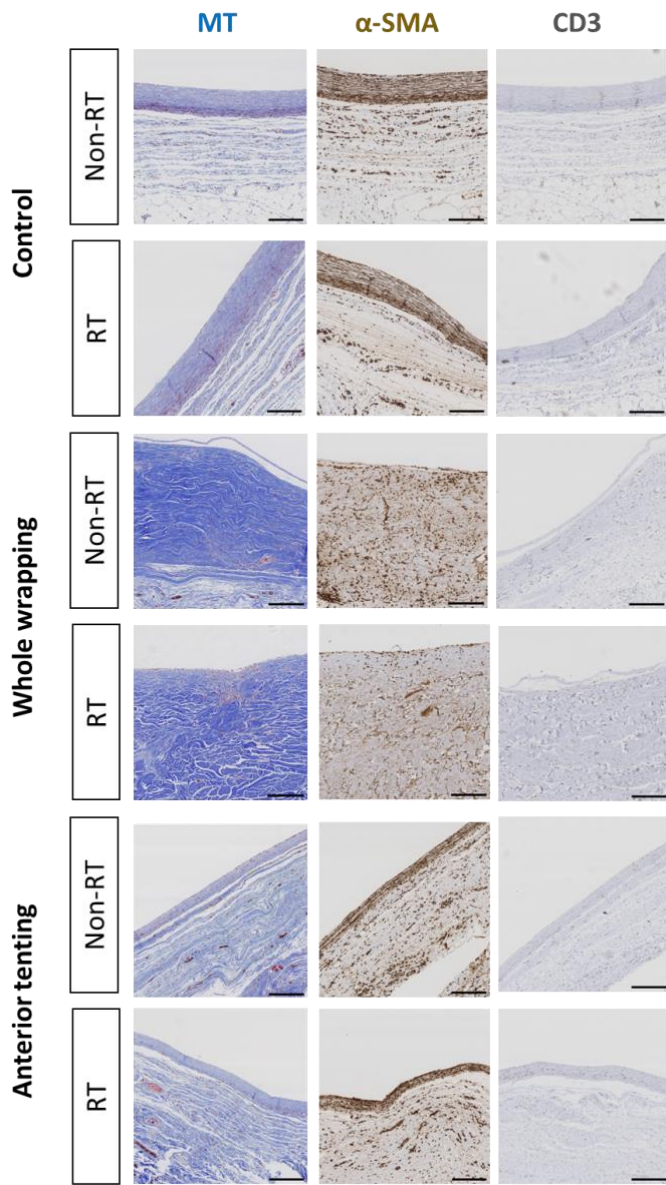
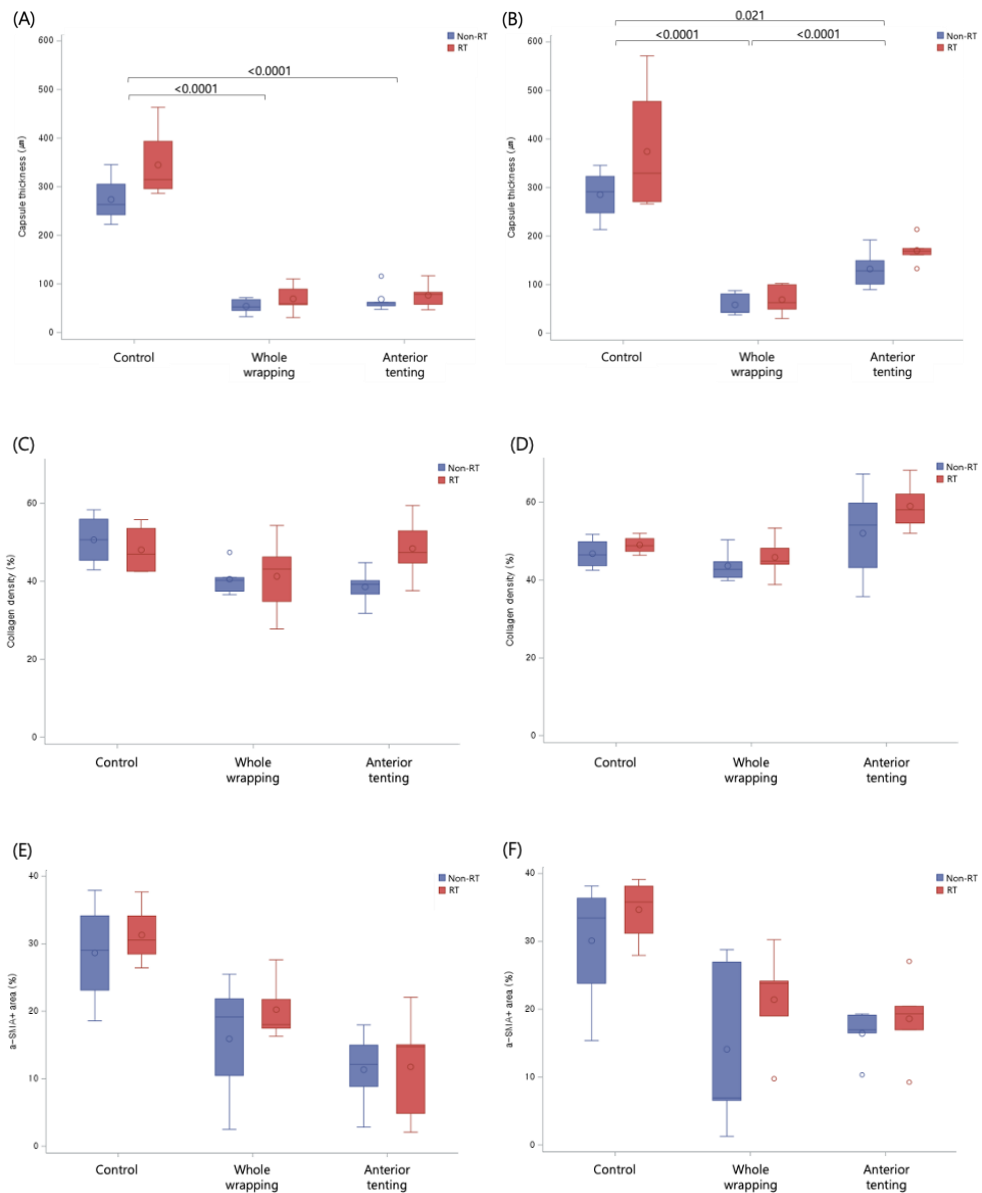


Figure 8. Masson' s trichrome staining and immunohistochemistry ( $\alpha$ -SMA and CD3) result of the implant capsule of posterior side in control (*first and second row*), whole wrapping (*third and fourth row*), and anterior tenting (*fifth and sixth row*). Scale bars = 200  $\mu$ m (RT, Irradiation; Non-RT, Non-Irradiation).



Scale bar: 200 $\mu$ m

Figure 9. Distribution of the cellular capsule characteristics with standard errors among groups. The capsule thickness of (A) anterior and (B) posterior side, collagen density of (C) anterior and (D) posterior side,  $\alpha$ -SMA positive area of (E) anterior and (F) posterior side, and CD3 positive cell count of (G) anterior and (H) posterior side (RT, Irradiation; Non-RT, Non-Irradiation).



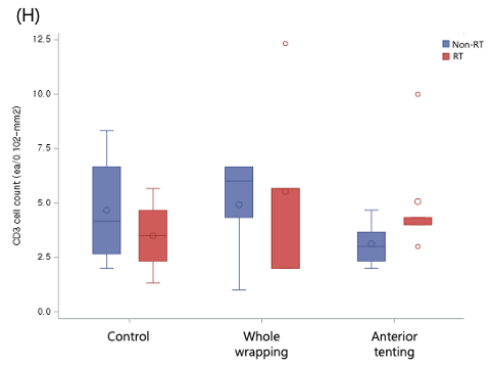
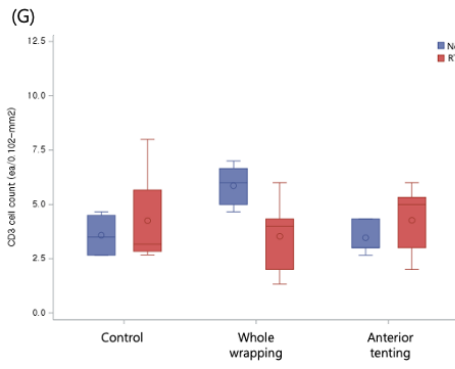


Figure 10. Distribution of the ADM characteristics with standard errors depending on the side from which ADM was harvested. (A) Total capsule thickness including ADM, (B) collagen density, (C)  $\alpha$ -SMA positive area and (D) CD3+ cell count of ADM (RT, Irradiation; Non-RT, Non-Irradiation).

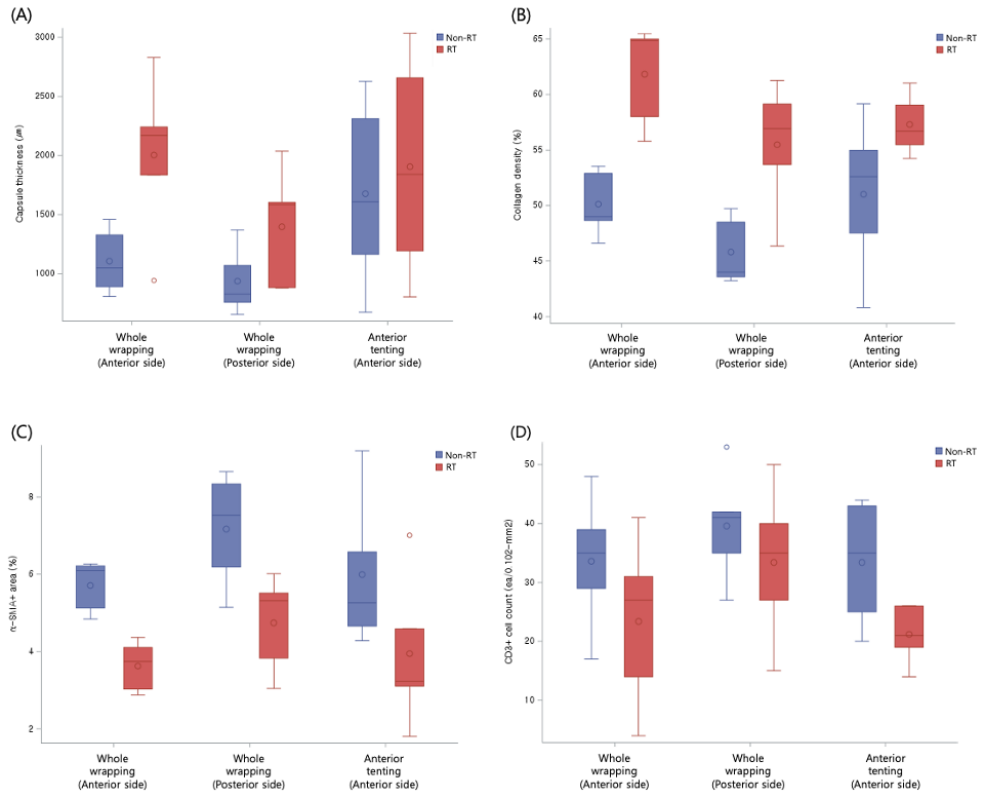


Table 1. Statistical result of cellular capsule characteristics among groups (RT, Irradiation; Non-RT, Non-Irradiation).

Orientation	Result	Radiation	Group		
			Control (n=4)	Whole wrapping (n=5)	Anterior tenting (n=5)
Anterior side	Capsule thickness ( $\mu\text{m}$ )	Non-RT	273.64 $\pm$ 51.72	53.89 $\pm$ 16.15	68.34 $\pm$ 27.19
		RT	344.71 $\pm$ 80.59	69.19 $\pm$ 30.80	76.57 $\pm$ 26.89
	Collagen density (%)	Non-RT	55.15 $\pm$ 15.53	37.49 $\pm$ 13.13	39.29 $\pm$ 11.14
		RT	60.95 $\pm$ 6.65	48.57 $\pm$ 11.29	54.33 $\pm$ 9.55
	$\alpha$ -SMA+ area (%)	Non-RT	20.74 $\pm$ 11.96	10.47 $\pm$ 5.90	11.35 $\pm$ 5.85
		RT	26.93 $\pm$ 10.40	13.06 $\pm$ 8.44	11.76 $\pm$ 8.18
CD3+ cell count (cells/0.01mm <sup>2</sup> )	Non-RT	12.41 $\pm$ 3.18	4.60 $\pm$ 4.47	3.60 $\pm$ 0.89	
	RT	14.16 $\pm$ 3.94	5.47 $\pm$ 2.76	4.47 $\pm$ 1.50	
Posterior side	Capsule thickness ( $\mu\text{m}$ )	Non-RT	285.42 $\pm$ 54.91	58.33 $\pm$ 23.87	132.10 $\pm$ 40.86
		RT	374.10 $\pm$ 141.77	68.88 $\pm$ 31.62	170.24 $\pm$ 29.06
	Collagen density (%)	Non-RT	48.53 $\pm$ 9.60	44.70 $\pm$ 6.81	52.03 $\pm$ 12.66
		RT	59.23 $\pm$ 9.67	49.84 $\pm$ 5.99	59.01 $\pm$ 6.39
	$\alpha$ -SMA+ area (%)	Non-RT	17.82 $\pm$ 10.39	6.93 $\pm$ 3.64	16.45 $\pm$ 3.64
		RT	28.99 $\pm$ 3.75	14.87 $\pm$ 11.83	18.61 $\pm$ 6.44
CD3+ cell count (cells/0.01mm <sup>2</sup> )	Non-RT	11.50 $\pm$ 4.36	4.20 $\pm$ 1.98	3.53 $\pm$ 1.50	
	RT	14.16 $\pm$ 4.25	7.60 $\pm$ 4.62	5.13 $\pm$ 3.10	

Table 2. Generalized Estimating Equations (GEE) of cellular capsule characteristics.

Orientation	Result	Effect		
		Group*Radiation	Group	Radiation
Anterior side	Capsule thickness	0.472	<b>0.029</b>	0.107
	Collagen density	0.241	0.112	0.289
	$\alpha$ -SMA+ area	0.611	0.164	0.246
	CD3+ cell count	0.097	0.371	0.581
Posterior side	Capsule thickness	0.331	<b>0.037</b>	0.067
	Collagen density	0.702	0.081	0.112
	$\alpha$ -SMA+ area	0.603	0.077	0.054
	CD3+ cell count	0.104	0.646	0.491

Table 3. Statistical result of ADM characteristics among groups (RTx, Irradiation; Non-RTx, Non-Irradiation).

Group	Result	Radiation	Orientation	
			Anterior side	Posterior side
Whole wrapping (n=5)	Total capsule thickness ( $\mu\text{m}$ )	Non-RT	1106.01 $\pm$ 280.21	936.18 $\pm$ 286.62
		RT	2004.09 $\pm$ 693.46	1396.78 $\pm$ 505.36
	Collagen density (%)	Non-RT	50.13 $\pm$ 2.96	45.81 $\pm$ 3.06
		RT	61.82 $\pm$ 4.57	55.47 $\pm$ 5.82
	$\alpha$ -SMA+ area (%)	Non-RT	5.71 $\pm$ 0.67	7.17 $\pm$ 1.48
		RT	3.63 $\pm$ 0.65	4.74 $\pm$ 1.25
Anterior tenting (n=5)	CD3+ cell count (cells/0.102mm <sup>2</sup> )	Non-RT	33.60 $\pm$ 11.57	39.60 $\pm$ 9.58
		RT	23.4 $\pm$ 14.54	33.40 $\pm$ 13.24
	Total capsule thickness ( $\mu\text{m}$ )	Non-RT	1677.38 $\pm$ 803.73	
		RT	1905.71 $\pm$ 944.78	
	Collagen density (%)	Non-RT	51.01 $\pm$ 7.08	
		RT	57.30 $\pm$ 2.73	
	$\alpha$ -SMA+ area (%)	Non-RT	6.00 $\pm$ 1.99	
		RT	3.95 $\pm$ 1.97	
	CD3+ cell count (cells/0.102mm <sup>2</sup> )	Non-RT	33.40 $\pm$ 10.69	
		RT	21.20 $\pm$ 5.07	

Table 4. Generalized Estimating Equations (GEE) of ADM characteristics

Result	Effect		
	Side*Radiation	Side	Radiation
Total capsule thickness	0.132	0.159	<b>0.024</b>
collagen density	0.134	0.157	<b>0.015</b>
$\alpha$ -SMA+ area	0.927	0.159	<b>0.009</b>
CD3+ cell count	0.103	0.09	<b>0.025</b>

## References

1. Siegel RL, Miller KD, Fuchs HE, Jemal A. Cancer statistics, 2021. *CA Cancer J Clin* 2021;71(1):7–33.
2. Rebowe RE, Allred LJ, Nahabedian MY. The evolution from subcutaneous to prepectoral prosthetic breast reconstruction. *Plast Reconstr Surg Glob Open* 2018;6(6):e1797.
3. Valero MG, Muhsen S, Moo TA, et al. Increase in utilization of nipple-sparing mastectomy for breast cancer: Indications, complications, and oncologic outcomes. *Ann Surg Oncol* 2020;27(2):344–351.
4. Petrie K, Cox CT, Becker BC, MacKay BJ. Clinical applications of acellular dermal matrices: A review. *Scars Burn Heal*. 2022;8:20595131211038313. Published 2022 Jan 19.
5. Cottler PS, Olenczak JB, Ning B et al. Fenestration improves acellular dermal matrix biointegration: An investigation of revascularization with photoacoustic microscopy. *Plast Reconstr Surg* 2019;143(4):971–981.
6. Kim IK, Park SO, Chang H, Jin US. Inhibition mechanism of acellular dermal matrix on capsule formation in expander-implant breast reconstruction after postmastectomy radiotherapy. *Ann Surg Oncol* 2018;25(8):2279–2287.
7. Namnoum JD, Moyer HR. The role of acellular dermal matrix in the treatment of capsular contracture. *Clin Plast Surg*. 2012;39(2):127–136.
8. Galdiero M, Larocca F, Iovene MR, et al. Microbial Evaluation in Capsular Contracture of Breast Implants [published correction appears in *Plast Reconstr Surg*. 2018 Mar;141(3):823.

9. Ajdic D, Zoghbi Y, Gerth D, Panthaki ZJ, Thaller S. The Relationship of Bacterial Biofilms and Capsular Contracture in Breast Implants. *Aesthet Surg J*. 2016;36(3):297–309.
10. de Kerckhove M, Iwahira Y. Risk Factors for Capsular Contracture: A Retrospective Study in Immediate Reconstruction versus Delayed Reconstruction. *Plast Reconstr Surg Glob Open*. 2020;8(5):e2864. Published 2020 May 21.
11. Sinnott C J, Persing S M, Pronovost M, Hodyl C, McConnell D, Ott Young A. Impact of postmastectomy radiation therapy in prepectoral versus subpectoral implant-based breast reconstruction. *Ann Surg Oncol*. 2018;25(10):2899–2908.
12. Cottler PS, Olenczak JB, Ning B, et al. Fenestration Improves Acellular Dermal Matrix Biointegration: An Investigation of Revascularization with Photoacoustic Microscopy. *Plast Reconstr Surg*. 2019;143(4):971–981.
13. Han WY, Han SJ, Eom JS, Kim EK, Han HH. "A Comparative Study of Wrap-Around versus Anterior Coverage Placement of Acellular Dermal Matrix in Prepectoral Breast Reconstruction" *Plast Reconstr Surg*. 2023 Mar 3. doi:10.1097/PRS.0000000000010347. Epub ahead of print.
14. Kong TH, Chung KJ, Kim T, Lee JH. Effect of acellular dermal matrix thickness and surface area on direct-to-implant breast reconstruction. *Gland Surg*. 2022;11(8):1301–1308.

15. Dubrovskaya VF, Chukhlovin AB. Planning trials with fibrosis-preventing agents. *Int J Radiat Oncol Biol Phys*. 2005;61: 307-309.
16. Eltze E, Schäfer U, Bettendorf O, et al. Radiation-induced capsule tissue reactions around textured breast implants in a rat model. *Breast* 2006;15(3):331-338.
17. Mulder JW, Nicolai J-PA. Breast tonometry: a practical device for accurate measurement of capsule-formation. *Eur J Plast Surg* 1990;13(6):274-277.
18. Moore JR. Applanation tonometry of breasts. *Plast Reconstr Surg* 1979;63(1):9-12.
19. Scheflan M, Allweis TM, Ben Yehuda D, Maisel Lotan A. Meshed acellular dermal matrix in immediate prepectoral implant-based breast reconstruction. *Plast Reconstr Surg Glob Open* 2020;8(11):e3265.
20. Gwak H, Jeon YW, Lim ST, Park SY, Suh YJ. Volume replacement with diced acellular dermal matrix in oncoplastic breast-conserving surgery: A prospective single-center experience. *World J Surg Oncol* 2020;18(1):60.
21. Spear SL, Sher SR, Al-Attar A, Pittman T. Applications of acellular dermal matrix in revision breast reconstruction surgery. *Plast Reconstr Surg*. 2014;133(1):1-10.
22. Stump A, Holton LH 3rd, Connor J, Harper JR, Slezak S, Silverman RP. The use of acellular dermal matrix to prevent capsule formation around implants in a primate model. *Plast Reconstr Surg* 2009;124(1):82-91.

23. Bui, J.M., Perry, T., Ren, C.D. et al. Histological Characterization of Human Breast Implant Capsules. *Aesth Plast Surg* 2015;39:306–315.
24. Kim HB, Han HH, Eom JS. Difference in the occurrence of capsular contracture according to the characteristics of the tissue in an irradiated rat model. *Plast Reconstr Surg.* 2023 Mar 8. doi: 10.1097/PRS.0000000000010387. Epub ahead of print.
25. Haran O, Bracha G, Tiosano A, et al. Postirradiation Capsular Contracture in Implant–Based Breast Reconstruction: Management and Outcome. *Plast Reconstr Surg.* 2021;147(1):11–19.
26. Komorowska–Timek E, Oberg KC, Timek TA, Gridley DS, Miles DAG. The effect of AlloDerm envelopes on periprosthetic capsule formation with and without radiation. *Plast Reconstr Surg.* 2009;123(3):807–816.
27. Ibrahim HZ, Kwiatkowski TJ, Montone KT, et al. Effects of external beam radiation on the allograft dermal implant. *Otolaryngol Head Neck Surg.* 2000;122:189–194.
28. Lee JH, Kim HG, Lee WJ. Characterization and tissue incorporation of cross–linked human acellular dermal matrix. *Biomaterials.* 2015;44:195–205.
29. Woo SJ, Ha JH, Jin US. Comparison of irradiated and non–irradiated acellular dermal matrices in breast reconstruction under radiotherapy. *Arch Plast Surg* 2021;48(1):33–43.

30. Hammond DC, Chaudhry A. Defining the Relationship between Pocket and Breast Implant Surface Area as the Basis for a New Classification System for Capsular Contracture. *Plast Reconstr Surg.* 2022;150(3):496–509.

31. Garcia O Jr, Scott JR. Analysis of acellular dermal matrix integration and revascularization following tissue expander breast reconstruction in a clinically relevant large–animal model. *Plast Reconstr Surg.* 2013;131:741e–51e.

# 초 록

## 방사선 조사 유방재건 랫드 모델에서 무세포성 진피 기질 피복 방법에 따른 비교

서울대학교 대학원

의학과 성형외과학 전공

김 지 영

### 연구 배경

무세포성 진피 기질 (Acellular dermal matrix)을 이용한 보형물 기반 유방재건술은 최근 선호되는 유방 재건 방법이다. 유방 재건 시 무세포성 진피 기질을 이용해 보형물을 감싸는 방법에는 여러 가지가 시도되었고, 대표적으로 Anterior tenting technique 과 Wrapping technique 이 있다. 이번 연구는 이 두 방법의 결과를 비교하고자 하였다.

### 연구 방법

15 마리의 쥐를 대상으로 실험을 수행하였다. 각 쥐에게는 직경 1.5cm 의 실리콘 보형물 두 개를 삽입하였다. 대조군에는 실리콘 보형물만 삽입하였으며, Anterior tenting 군에는 보형물의 앞면을 무세포성 진피 기질로 덮었고, Whole wrapping 군에서는 보형물의 모든 면을 무세포성 진피 기질로 덮은 후 실험 동물에 삽입하였다. 수술 후 3 주째 한쪽 보형물에 임의로 방사선을 조사하였으며, 수술 후 3 개월째 Tonometer 를

이용하여 보형물 주머니 내의 압력을 측정하고, 무세포성 진피 기질과 피막을 함께 검체를 채취하여 조직학적 검사를 수행하였다.

## 연구 결과

대조군의 쥐 한 마리가 조기 폐사하여 총 14 마리에 대해 결과 분석 시행하였다. Anterior tenting technique 에 비해 Whole wrapping 을 한 경우, Tonometer 값의 변화 폭이 유의하게 더 컸다 ( $p=0.008$ ). 무세포성 진피 기질로 덮힌 면의 세포성 피막은 유의하게 그 두께가 얇았고 (앞면,  $p=0.029$ ; 뒷면,  $p=0.037$ ), 다른 세포성 피막의 특성은 조직학적으로 유의한 차이가 없었다. 무세포성 진피 기질을 분석한 결과, 방사선 조사한 경우 전체 피막 두께 ( $p=0.024$ )와 콜라겐 밀도 ( $p=0.015$ )가 유의하게 증가하였으며,  $\alpha$ -SMA 양성 영역 ( $p=0.009$ )과 CD3 양성 세포 수 ( $p=0.025$ )는 유의하게 감소하였다.

## 결론

Whole wrapping technique 은 anterior tenting technique 에 비해 방사선에 의한 무세포성 진피 기질의 구조적 변화에 따른 보형물 주머니 내압 증가폭이 크다. 따라서, 무세포성 진피 기질을 이용한 보형물 기반 유방재건에서 수술 후 방사선 치료 가능성이 있는 환자들에게는 whole wrapping 보다는 anterior tenting technique 을 권장한다.

**주요어 :** 유방재건, 무세포성 진피 기질, 방사선, 피막 구축

**학 번 :** 2021-29067